ICASSP 2021 - 2021 IEEE International Conference on Acoustics, Speech and Signal Processing (ICASSP) | 978-1-7281-7605-5/20/$31.00 ©2021 IEEE | DOI: 10.1109/ICASSP39728.2021.9415108

TCLA ARRAY: A NEW SPARSE ARRAY DESIGN WITH LESS MUTUAL COUPLING

Ahmed M. A. Shaalan, Jun Du†, Yan-Hui Tu

University of Science and Technology of China, Hefei, China
ShaalanAhmed@outlook.com, ✉ jundu@ustc.edu.cn, tuyanhui@ustc.edu.cn

ABSTRACT

The recent criteria of a preferable linear sparse array for a robust direction of arrival (DOA) estimation are the closed-form expression for its sensor locations, the large central uniform linear array (ULA) segment in its resulting co-array and the fewer sensor pairs with small separations in its configuration. This paper aims to introduce a new proposed sparse array that takes into account all these considerations. The new sparse array configuration is proposed based on utilizing the two coordinates of a linear axis (TCLA) to situate its sub-arrays. Compared to the (super) nested array having the same sensor number, the TCLA array owns the same number of uniform degrees of freedom (DOFs) but possesses less mutual coupling effects. These properties are quantitatively covered, and numerical simulations are included to demonstrate the superior performance of the proposed array.

Index Terms—

Super nested arrays, TCLA arrays, difference co-arrays, mutual coupling, DOA estimation

1. INTRODUCTION

In array processing, the problem of detecting more signals than the number of physical sensors being used still remains at the very heart of various applications [1]-[3]. Compared to uniform linear arrays (ULAs), minimum redundancy arrays (MRAs) [4], [5], and minimum hole arrays (MHAs) [6], grouped under the umbrella of traditional linear sparse arrays, could achieve a higher number of degrees-of-freedom (DOFs) in their virtual difference co-array, thereby detecting more sources than the number of actual sensors. However, they have no closed-form expressions for their sensor locations, nor for their obtainable DOFs.

Recently, new sparse arrays such as co-prime arrays (CPAs) [7], [8] and nested arrays (NAs) [9] have resurrected the interest in this field and have invited researchers to revisit this topic, since they feature a systematic development for their sensor locations and the achievable DOFs. As a result, many developed arrays out of these two basic array configurations have shown up, including but not limited to, generalized co-prime arrays [10], thinned co-prime arrays (TCAs) [11], optimized co-prime arrays (OpCAs) [12], improved nested arrays [13] and augmented nested arrays [14].

In practice, with considering mutual coupling [15], [16], these recent sparse arrays - as they adopt nonuniform inter-sensor spacings - have also come as one of state-of-the-art solutions to alleviate it compared to ULAs. However, they still have their own shortcomings, e.g., co-prime-array-based arrays have a smaller ULA part, $\mathbb{U}$, in the co-array domain, $\mathbb{D}$, in comparison with nested-array-based arrays, while these latter arrays, in contrast, have dense ULA sections in their physical configuration, resulting in higher mutual coupling than in those former. Thus, to tackle these problems, a super nested array (SNA) [17], [18], has been proposed to possess the same uniform capacity as does its parent nested array, and at the same time to achieve less mutual coupling in comparison.

Motivated by building a new sparse array configuration which has a considerable uniform capacity and much less severe mutual coupling effects compared to the existing sparse arrays, this paper aims to introduce such a new array geometry constructed based on exploiting the two coordinates of a linear axis (TCLA) to locate its constituent sub-arrays. Generally, The TCLA array configuration is composed of three sub-arrays. The first sub-array is arranged along the negative coordinate while the other two are placed on the positive one. With such an arrangement, TCLA arrays yield a virtual co-array having the same ULA part as the nested and super nested arrays do, but has smaller weight functions, thereby having less severe mutual coupling effects than in both.

The reminder of this paper is organized as follows. Section 2 reviews sparse array processing and mutual coupling models. TCLA arrays are then introduced in Section 3. In Section 4, we highlight the properties of the co-array of the TCLA array. The improved performance of TCLA arrays under mutual coupling will be demonstrated in Section 5.

2. SPARSE ARRAY SIGNAL PROCESSING

2.1. The Mathematical Model

Throughout this section, $(\cdot)^\top$, $(\cdot)^*$ and $(\cdot)^H$ denote the transpose, complex conjugate and conjugate transpose operators, respectively. $\odot$ and $\otimes$ imply the Khatri-Rao product and Kronecker product, respectively. $vec(\cdot)$ refers to the vectorization

operator.

Assume that the number of incoming signals, K, with their corresponding complex amplitudes, written as $s_k, k = 1, ..., K$, and their angles of arrivals, denoted as $[\theta_1, \theta_2, ..., \theta_K]$ in the range $[-\pi/2, \pi/2]$, are being intercepted by a sparse array of N actual sensors. These sensors are located according to specific closed-from expressions at these positions $\rho_i d$, where ρ_i belongs to some integer set $\mathbb{P}$ and d, representing the minimum distance between sensors, is half of the wavelength of the received signal, $d = \lambda/2$. Then, the measurement vector $\mathbf{z}_{\mathbb{P}}$, made by these sensors, at a time instant, t, is:

$$\mathbf{z}_{\mathbb{P}}(t) = \sum_{k=1}^{K} \mathbf{a}(\theta_k) s_k(t) + \mathbf{n}_{\mathbb{P}}(t) = \mathbf{A}\mathbf{s}(t) + \mathbf{n}_{\mathbb{P}}(t), \quad (1)$$

where $\mathbf{a}(\theta_k) = \{e^{j2\pi\rho_i\bar{\theta}_k},\ \rho_i \in \mathbb{P},\ i = 1, .., N\}$ is the array steering vector corresponding to the k-th signal direction, θ_k, whereas $\bar{\theta}_k = (d/\lambda)\sin\theta_k$ is this direction normalized value, $\mathbf{A} = [\mathbf{a}(\theta_1),\ ..., \mathbf{a}(\theta_K)]$ is the array steering matrix, and $\mathbf{s}(t) = [s_1(t),\ ..., s_K(t)]$ is the source vector of size $(K \times 1)$ with every s_k distributed as $\mathcal{CN}(0, \sigma_k^2)$ and is considered uncorrelated from the other. The entries of of the noise vector $\mathbf{n}_{\mathbb{P}}(t)$ are assumed to be (i.i.d.) random variables following the complex Gaussian distribution $\mathcal{CN}(0, \sigma^2)$, as well.

Thus, as such, the covariance matrix of data vector $\mathbf{z}_{\mathbb{P}}$ with suppressing the time dependence in Eq. (1) to simplify the notation is obtained as

$$\mathbf{R}_{\mathbf{zz}} = E[\mathbf{z}_{\mathbb{P}}\mathbf{z}_{\mathbb{P}}^H] = A\mathbf{R}_{\mathbf{ss}}A^H + \mathbf{R}_{\mathbf{nn}} = \sum_{k=1}^{K} \sigma_k^2 \mathbf{a}(\theta_k)\mathbf{a}^H(\theta_k) + \sigma^2\mathbf{I}_{\mathbf{n}}, \quad (2)$$

where $\mathbf{R}_{\mathbf{ss}} = E[\mathbf{s}\mathbf{s}^H] = diag([\sigma_1^2, ..., \sigma_K^2])$ is the source covariance matrix, with σ_k^2 denoting the power of the source k-th and $\mathbf{R}_{\mathbf{nn}} = E[\mathbf{n}_{\mathbb{P}}\mathbf{n}_{\mathbb{P}}^H]$ is the noise covariance matrix. In practice, the covariance matrix is estimated using the available T samples, i.e.,

$$\hat{\mathbf{R}}_{\mathbf{zz}} = \frac{1}{T}\sum_{t=1}^{T} \mathbf{z}_{\mathbb{P}}(t)\mathbf{z}_{\mathbb{P}}^H(t). \quad (3)$$

Vectorizing $\mathbf{R}_{\mathbf{zz}}$ yields an $(N^2 \times 1)$ column vector that can be expressed as:

$$\mathbf{z}_{\mathbf{vec}} = vec(\mathbf{R}_{\mathbf{zz}}) = \tilde{\mathbf{A}}(\theta_1, \theta_2, \cdots, \theta_K)\tilde{\mathbf{s}}_k + \sigma^2\tilde{\mathbf{I}}_{\mathbf{n}}, \quad (4)$$

where $\mathbf{A} \odot \mathbf{A}^H = \tilde{\mathbf{A}} = [\tilde{a}(\theta_1),\ ...,\ \tilde{a}(\theta_K)] = [a(\theta_1) \otimes a(\theta_1)^*,\ ...,\ a(\theta_K) \otimes a(\theta_K)^*]$, $\tilde{\mathbf{s}}_k$ is the source vector, and $\tilde{\mathbf{I}}_{\mathbf{n}} = vec[\mathbf{I}_{\mathbf{n}}] = [\mathbf{e}_1^\top, \mathbf{e}_2^\top, \cdots, \mathbf{e}_N^\top]^\top$ with $\mathbf{e}_i$ referring to a vector of all zeros except for the corresponding main diagonal element, i-th, of $\mathbf{I}_{\mathbf{n}}$, which equals one. Comparing Eq. (1) with Eq. (4), we see that $\mathbf{z}_{\mathbf{vec}}$ behaves like a measurement vector that is made by a virtual array whose steering vector is $\tilde{\mathbf{a}}(\theta_k)$ for virtual sensors located at $\tilde{\rho}_i d$, where $\tilde{\rho}_i \in \mathbb{D}$, $i = 1,\ ...,\ N^2$ and $\mathbb{D}$ is the virtual counterpart of $\mathbb{P}$. The data vector $\mathbf{z}_{\mathbb{U}}$ corresponding to the central set of the adjacent sensors, $\mathbb{U}$, of $\mathbb{D}$ and bounded by $\pm\tilde{\rho}_{\mathbb{U}}$ is subsequently extracted as follows:

$$\mathbf{z}_{\mathbb{U}} = \frac{1}{w(\tilde{\rho})}\sum_{\tilde{\rho}=-\tilde{\rho}_{\mathbb{U}}}^{\tilde{\rho}_{\mathbb{U}}} \mathbf{z}_{\mathbf{vec}}(\tilde{\rho}), \quad (5)$$

where the weight function of the virtual sensor $\tilde{\rho}$, $w(\tilde{\rho})$, is defined as the number of actual sensor pairs that lead to it and can be found as $w(\tilde{\rho}) = \{(\rho_i, \rho_j) \in \mathbb{P}^2 \mid \rho_i - \rho_j = \tilde{\rho}\}$.

2.2. Mutual Coupling

The observation vector in Eq. (1) is based on some strict assumptions, among which the exclusion of the mutual coupling effect. In practice, the mutual coupling is observed to exist in between the array sensors. Therefore, the mutual coupling is inevitably incorporated into Eq. (1) as

$$\mathbf{z}_{\mathbb{P}}(t) = \mathbf{C}\mathbf{A}\mathbf{s}(t) + \mathbf{n}_{\mathbb{P}}(t), \quad (6)$$

where $\mathbf{C}$ is the $(N \times N)$ mutual coupling matrix that can be modeled in terms of many factors, among which the distance between the array sensors. According to [16], [19]-[21], $\mathbf{C}$ can be approximated by a B-banded symmetric Toeplitz matrix in the ULA configuration as follows:

$$\mathbf{C}(\tilde{\rho}) = \begin{cases} \mathbf{c}_{|\tilde{\rho}|}, & |\tilde{\rho}| \le B, \\ 0, & otherwise, \end{cases} \quad (7)$$

where its entry $\mathbf{c}_{\tilde{\rho}}$ is considered as a function of only the sensor separation, $\tilde{\rho}$, and is empirically found to be inversely proportional to this separation in the way that $1 = \mathbf{c}_0 > |\mathbf{c}_{\tilde{\rho}=1}| > |\mathbf{c}_2| > \cdots > |\mathbf{c}_{\tilde{\rho}=B}| > |\mathbf{c}_{B+1} \mid = 0$ [19]. Thus, the coupling coefficients used in [17] are as follows: $\mathbf{c}_1 = \mathbf{c}e^{j\pi/3}$, and $\mathbf{c}_i = \mathbf{c}_1 e^{-j(\tilde{\rho}-1)\pi/8}/\tilde{\rho}$, where the parameter $\mathbf{c}$ can take a value in the range [0.1 : 1].

3. SENSOR LOCATIONS IN TCLA ARRAYS

In this section, we introduce the TCLA array geometry using Definition 1, and then we illustrate its design process with the aid of Fig. 1, which, in accordance with Definition 1, depicts the prospective of employing the two parts of a linear axis to locate its sub-arrays.

Definition 1 (TCLA Array Configuration): Assume that N^o is obtained from the nested array optimal parameter N_1 as in Table 1, and N^t and N^e are afterwards determined as $N^o - 1$, and $N - 2N^o + 1$ in sequential, TCAL arrays are, then, specified by the integer set $\mathbb{P}$, defined by

$$\mathbb{P} = \{\mathbb{P}_1 \cup \mathbb{P}_2 \cup \mathbb{P}_3\},$$

where

$$\mathbb{P}_1 = \{\rho_i^o, 1 \le i \le N^o\} = \{-(1 + 2\ell_o)\ |0 \le \ell_o \le N^o - 1\},$$
$$\mathbb{P}_2 = \{\rho_i^e, 1 \le i \le N^e\} = \{(\ell_{NP}\ell_e)\ |0 \le \ell_e \le N^e - 1\},$$
$$\mathbb{P}_3 = \{\rho_i^t, 1 \le i \le N^t\} = \{\ell_{NP}(N^e - 1) + 2\ell_t\ |1 \le \ell_t \le N^t\}.$$

Table 1: General closed-form expressions for distributing N into optimal N_1, N_2 for nested arrays and optimal N^o for TCLA arrays.

	NA		TCLA array
N	N_1	N_2	N^o
even	$N/2$ (odd)	$N/2$	$(N_1+1)/2$
even	$N/2$ (even)	$N/2$	$N_1/2$
odd	$(N-1)/2$ (odd)	$(N+1)/2$	$(N_1+1)/2$
odd	$(N-1)/2$ (even)	$(N+1)/2$	$(N_1+2)/2$

ℓ_{NP} is fixed equal to $2N^o$, and the sets $\mathbb{P}_1$, $\mathbb{P}_2$ and $\mathbb{P}_3$ represent the positions of sensors in the 1st, 2nd and 3rd sub-arrays, respectively, which constitute the TCLA array configuration.

As an example, let's consider the TCLA array configuration with $N = 8$ (number of actual sensors), which, according to the second row of Table 1, is distributed into $N^o = N_1/2 = 4/2 = 2$, and consequently $N^t = N^o - 1 = 2 - 1 = 1$ and $N^e = N - 2N^o + 1 = 5$. Setting $N^o = 2$ in Definition 1 closed-form expression $\{-(1+2\ell_o)d \mid 0 \le \ell_o \le N^o - 1\}$ yields $\mathbb{P}_1 = \{-3, -1\}$ while setting $N^e = 5$ with $\ell_{NP} = 4$ and $N^t = 1$ in their corresponding expressions in Definition 1 gives $\mathbb{P}_2 = \{0, 4, 8, 12, 16\}$ and $\mathbb{P}_3 = \{18\}$, respectively. Having the union of these sub-arrays (as in Definition 1) leads to the TCLA array configuration shown in the top of Fig. 1.

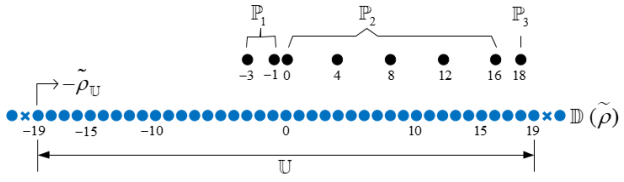

Fig. 1: The physical geometry and difference co-array of a TCLA array with $N^o = 2$, $N^t = 1$ and $N^e = 5$, where black/blue bullets denote actual/virtual sensors, and crosses indicate holes (or equivalently "missing virtual sensors").

4. CO-ARRAY PROPERTIES

The importance of TCLA arrays arises from two properties given below in Proposition 1 and Eq. (8).

Proposition 1: The TCLA array features a difference co-array, $\mathbb{D}$, that has a central ULA part, $\mathbb{U}$, in the range $[-(2N^eN^o - 1),\ 2N^eN^o - 1]$, where $2N^eN^o - 1$ represents its one-side number of uniform DOFs, $\tilde{\rho}_{\mathbb{U}}$.

Proof: The proof is available in Section 7.

Concretely, for the TCLA array with $N = 8$ while being distributed, by Table 1, into $N^o = 2$, $N^t = 1$ and $N^e = 5$, its uniform capacity, $\mathbb{U}$, in accordance with Proposition 1 is in the range $[-19, 19]$, where 19 is its $\tilde{\rho}_{\mathbb{U}}$, as it can be seen from the bottom of Fig. 1. For comparison, the super nested array (SNA) has the same co-array as its parent nested array, and as their equal $\tilde{\rho}_{\mathbb{U}}$ is expressed as $N_2(N_1+1) - 1$, with the distribution $N_1 = N_2 = 4$ of $N = 8$ (as in Table 1), we see that the three arrays do enjoy the same exact uniform capacity.

However, in terms of the weight function $w(\tilde{\rho})$, which matters most for mutual coupling effects, especially at small spacings $w(1)$, $w(2)$ and $w(3)$, which empirically have a major impact on the mutual coupling of an array, the TCLA array sets itself apart from those two arrays. More specifically, according to the definition of the weight function and the TCLA array configuration stated in Definition 1, the numbers of sensors with separations 1, 2, and 3 are the weight function $w(1)$, $w(2)$ and $w(3)$, respectively. Therefore, for a TCLA array, its weight function $w(\tilde{\rho})$ at $\tilde{\rho} = 1, 2, 3$ is

$$w(1) = 1,\ w(2) = N^o + N^t - 1,\ w(3) = 1, \tag{8}$$

and contrast this with NA and SNA whose first three weight functions are as follows:

Nested Array:

$$w(1) = N_1,\ w(2) = N_1 - 1,\ w(3) = N_1 - 2. \tag{9}$$

Super Nested Array:

$$w(1) = \begin{cases} 2,\ if\ N_1\ is\ even \\ 1,\ if\ N_1\ is\ odd, \end{cases} \tag{10}$$

$$w(2) = \begin{cases} N_1 - 3,\ if\ N_1\ is\ even \\ N_1 - 1,\ if\ N_1\ is\ odd, \end{cases} \tag{11}$$

$$w(3) = \begin{cases} 3,\ if\ N_1 = 4,\ 6 \\ 4,\ if\ N_1\ is\ even, \\ 1,\ if\ N_1\ is\ odd, \end{cases} \tag{12}$$

where N_1, N_2 are for both nested and super nested arrays. It can be seen that, unlike the NA (whose first weights increase as N_1 increases) and SNA, $w(1)$ and $w(3)$ for the TCLA array are always one regardless of the value of N.

More illustratively, with $N = 8$, the first three weight functions for the nested array, super nested array and TCLA array (in accordance with Eq. (9), Eqs. (10-12), Eq. (8)) are (4, 3, 2); (2, 1, 3); and (1, 2, 1), respectively. Therefore, it can be readily observed that the proposed TCLA array in comparison with the other two tested arrays has smaller weights, implying the existence of fewer sensor pairs with small separations; thereby, the less mutual coupling effect it is expected to experience - as it will be shown next.

5. NUMERICAL RESULTS

In this section, we compare the direction of arrival estimation performance in the presence of mutual coupling among nested arrays, super nested arrays, and TCLA arrays. The number of sensors is 12 for each array. The sensor locations for NA,

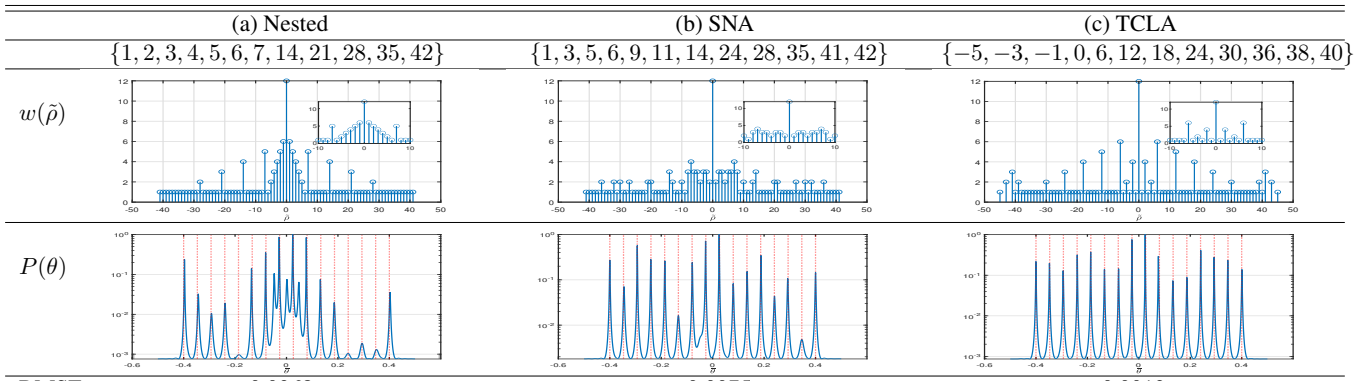

Fig. 2: Comparison among (a) nested array, (b) super nested array, and (c) TCLA array in the presence of mutual coupling. The MUSIC spectra $P(\bar{\theta})$ are computed under 0 dB SNR, 1000 snapshots, 12 sensors, and $K = 16$ sources, as indicated by red vertical lines. The mutual coupling model (7) has $c_1 = 0.3e^{j\pi/3}$, $c_i = c_1 e^{-j(i-1)\pi/8}/i$, and $B = 50$.

SNA, and TCLA array are listed in the first row of Fig. 2, respectively.

The second row in Fig. 2 visually illustrates each array co-array, together with the associated weight function. It can be observed that the three arrays have the same uniform capacity, ranging from -41 to 41. In addition, the weight function $w(1)$ for the nested array, super nested array, and TCLA array is 6, 2, and 1, respectively, which is also in accordance with Eq. (9), Eq. (10) and Eq. (8).

The third row of Fig. 2 demonstrates the MUSIC spectrum $P(\bar{\theta})$ [22] for various array configurations. For these spectra, the parameters are 0 dB SNR, 1000 snapshots, and $K = 16$ uncorrelated sources (> number of sensors, 12), located at $\bar{\theta}_i = -0.4 + 0.8(i-1)/(K-1)$ for $1 \le i \le K$. The mutual coupling model is based on Eq. (7) with $c_1 = 0.3e^{j\pi/3}$, $B = 50$ and $c_i = c_1 e^{-j(i-1)\pi/8}/i$ for $2 \le i \le B$. The spatial smoothing algorithm [23] or its alternative in [24], is evaluated directly from $\mathbf{z}_{\mathbb{U}}$ in Eq. (5) without using any decoupling algorithms.

From the third row of Fig. 2, it can be seen that the nested array has false peaks and some of the targets are almost missed, and that the SNA is struggling to exhibit all sources correctly. The TCLA array, by contrast, robustly displays 16 true peaks. Moreover, in terms of the estimation accuracy reflected by the root-mean-squared error (RMSE), which is defined as $RMSE = (\sum_{i=1}^{K}(\hat{\bar{\theta}}_k - \bar{\theta}_k)^2/K)^{1/2}$, where $\hat{\bar{\theta}}_k$ is the estimated normalized DOA of the k-th source calculated from the root MUSIC algorithm [25], and $\bar{\theta}_k$ is the true normalized DOA, it can be observed that the RMSE for the TCLA array (RMSE = 0.0013) is way less than that of the nested and super nested arrays. This can be attributed to its less mutual coupling deduced from its less mutual coupling leakage (shown in the fifth row of Fig. 2), which is found as $\mathcal{L} = ||\mathbf{C} - diag(\mathbf{C})||_F / ||\mathbf{C}||_F$, where $||\cdot||_F$ is the Frobenius norm of the mutual coupling matrix $\mathbf{C}$ [17].

6. CONCLUDING REMARKS

A new sparse array, that considered the most desirable features of the recently proposed sparse arrays, has been introduced. The proposed perspective of situating its sub-arrays ensured that its co-array has a considerable number of uniform DOFs, and its configuration is sparser in the sense that it has fewer sensor pairs with small separations.

7. APPENDIX: PROOF OF PROPOSITION 1

Proof: The statement that the TCLA $\mathbb{D}$ has $\mathbb{U}$ in the range $[-(2N^eN^o-1),\ 2N^eN^o-1]$ is equivalent to the following argument: for $\tilde{\rho}$ in the range $[-(2N^eN^o-1),\ 2N^eN^o-1]$, there is at least one pair of sensors leads to it, and as it is pretty known that $\mathbb{D}$ is a symmetric set, then finding $0 \le \tilde{\rho} \le 2N^oN^e - 1$ is an enough condition.

Therefore, for the odd numbers of $\tilde{\rho}$ starting from 1 to $2N^eN^o - 1$, it can be verified that they can be collected by $diff(\mathbb{P}_2, \mathbb{P}_1) = (\{\ell_{NP}\ell_e | 0 \le \ell_e \le N^e - 1\} - \{-(1 + 2\ell_o) | 0 \le \ell_o \le N^o - 1\}) = \{1 + 2\ell | 0 \le \ell \le N^eN^o - 1\} = \{\tilde{\rho}_i^{21}, 1 \le i \le N^eN^o\}$, while for the even numbers of $\tilde{\rho}$ starting from 0 to $2N^eN^o - 2$, they can be included by $diff(\mathbb{P}_2, \mathbb{P}_2) \cup diff(\mathbb{P}_3, \mathbb{P}_2) = \{\tilde{\rho}_i^{22}, 1 \le i \le N^e\} \cup \{\tilde{\rho}_i^{32}, 1 \le i \le N^eN^t\} = \{\ell_{NP}\ell_e | 0 \le \ell_e \le N^e - 1\} \cup \{(2+2\ell_t) + \ell_{NP}\ell_e | 0 \le \ell_t \le N^t - 1, 0 \le \ell_e \le N^e - 1\}$. Consequently, the union of $diff(\mathbb{P}_2, \mathbb{P}_1)$ and $diff(\mathbb{P}_2, \mathbb{P}_2) \cup diff(\mathbb{P}_3, \mathbb{P}_2)$ covers all the consecutive integers from 0 to $2N^eN^o - 1$.

8. ACKNOWLEDGMENT

This work was supported in part by the National Key R&D Program of China under contract No. 2017YFB1002202. This work was also funded by Tencent.

9. REFERENCES

[1] H. L.Van Trees, *Optimum Array Processing: Part IV of Detection, Estimation, and Modulation Theory*. New York, NY, USA: Wiley-Interscience, 2002.

[2] S. Pillai, *Array Signal Processing*. New York, NY, USA: Springer, 1989.

[3] R. T. Hoctor and C Kassam, "The unifying role of the coarray in aperture synthesis for coherent and incoherent imaging," *Proc. IEEE*, vol. 78, no. 4, pp. 735–752, April 1990.

[4] A. Moffet, "Minimum-redundancy linear arrays," *IEEE Trans. Antennas Propag.*, vol. AP-16, no. 2, pp. 172–175, Mar. 1968.

[5] M. Ishiguro, "Minimum redundancy linear arrays for a large number of antennas," Radio Sci., vol. 15, no. 6, pp. 1163–1170, 1980.

[6] G. S. Bloom and S.W. Golomb, "Application of numbered undirected graphs," *Proc. IEEE*, vol. 65, no. 4, pp. 562–570, April 1977.

[7] P. P. Vaidyanathan and P. Pal, "Sparse sensing with coprime samplers and arrays," *IEEE Trans. Signal Process.*, vol. 59, no. 2, pp. 573–586, Feb. 2011.

[8] P. Pal and P. P. Vaidyanathan, "Coprime sampling and the MUSIC algorithm," in *Proc. IEEE Dig. Signal Process. Educ. Workshop*, Jan. 2011, pp. 289–294.

[9] P. Pal and P. Vaidyanathan, "Nested arrays: A novel approach to array processing with enhanced degrees of freedom," *IEEE Trans. Signal Process.*, vol. 58, no. 8, pp. 4167–4181, Aug. 2010.

[10] S. Qin, Y. D. Zhang, and M. G. Amin, "Generalized coprime array configurations for direction-of-arrival estimation," *IEEE Trans. Signal Process.*, vol. 63, no. 6, pp. 1377–1390, Mar. 2015.

[11] A. Raza, W. Liu and Q. Shen, "Thinned Coprime Array for Second-Order Difference Co-Array Generation With Reduced Mutual Coupling," in *IEEE Transactions on Signal Processing*, vol. 67, no. 8, pp. 2052-2065, 15 April15, 2019.

[12] A. M. A. Shaalan and X. Yu, "DOA estimation based on the optimized coprime array configuration," *IEEE Access*, vol. 7, pp. 38789–38797,2019.

[13] M. Yang, L. Sun, X. Yuan, and B. Chen, "Improved nested array with hole-free DCA and more degrees of freedom," *Electron. Lett.*, vol. 52, no. 25, pp. 2068–2070, Dec. 2016.

[14] J. Liu, Y. Zhang, Y. Lu, S. Ren, and S. Cao, "Augmented nested arrays with enhanced DOF and reduced mutual coupling," *IEEE Trans. Signal Process.*, vol. 65, no. 21, pp. 5549–5553, Nov. 2017.

[15] M. I. Skolnik, *Introduction to Radar Systems*, 3rd ed. New York, NY, USA: McGraw Hill, 2001.

[16] C. A. Balanis, *Antenna Theory: Analysis and Design*, 4th ed. New York, NY, USA: Wiley, 2016.

[17] C. L. Liu and P. P.Vaidyanathan, "Super nested arrays: Linear sparse arrays with reduced mutual coupling—Part I: Fundamentals," *IEEE Trans. Signal Process.*, vol. 64, no. 15, pp. 3997–4012, Aug. 2016.

[18] C. L. Liu and P. P. Vaidyanathan, "Super nested arrays: Sparse arrays with less mutual coupling than nested arrays," in *Proc. IEEE Int. Conf. Acoust. ,Speech, Signal Process.*, Mar. 2016, pp. 2976–2980.

[19] B. Friedlander and A. Weiss, "Direction finding in the presence of mutual coupling," *IEEE Trans. Antennas Propag.*, vol. 39, no. 3, pp. 273–284, Mar 1991.

[20] B. Liao, Z. G. Zhang, and S. C. Chan, "DOA estimation and tracking of ULAs with mutual coupling," *IEEE Trans. Aerosp. Electron. Syst.*, vol. 48, no. 1, pp. 891–905, Jan. 2012.

[21] Z. Ye, J. Dai, X. Xu, and X.Wu, "DOA estimation for uniform linear array with mutual coupling," *IEEE Trans. Aerosp. Electron. Syst.*, vol. 45, no. 1, pp. 280–288, Jan. 2009.

[22] R. O. Schmidt, "Multiple emitter location and signal parameter estimation," *IEEE Trans. Antennas Propag.*, vol. 34, no. 3, pp. 276–280, Mar. 1986.

[23] T.-J. Shan, M. Wax, and T. Kailath, "On spatial smoothing for direction-of-arrival estimation of coherent signals," *IEEE Trans. Acoust., Speech Signal Process.*, vol. 33, no. 4, pp. 806–811, Aug. 1985.

[24] C.-L. Liu and P. P. Vaidyanathan, "Remarks on the spatial smoothing step in coarray MUSIC," *IEEE Signal Process. Lett.*, vol. 22, no. 9, pp. 1438–1442, Sep. 2015.

[25] Barabell, A., "Improving the Resolution of Eigenstructure-Based Direction-Finding Algorithms," *Proceedings of ICASSP*, Boston, MA, pp. 336–339, 1983.